

Association of Age at Diagnosis and Genetic Mutations in Patients With Neuroblastoma

Nai-Kong V. Cheung, MD, PhD

Jinghui Zhang, PhD

Charles Lu, PhD

Matthew Parker, PhD

Armita Bahrami, MD

Satish K. Tickoo, MD

Adriana Heguy, PhD

Alberto S. Pappo, MD

Sara Federico, MD

James Dalton, BS

Irene Y. Cheung, ScD

Li Ding, PhD

Robert Fulton, MS

Jianmin Wang, PhD

Xiang Chen, PhD

Jared Becksfort, MS

Jianrong Wu, PhD

Catherine A. Billups, MS

David Ellison, MD, PhD

Elaine R. Mardis, PhD

Richard K. Wilson, PhD

James R. Downing, MD

Michael A. Dyer, PhD

for the St Jude Children's Research
Hospital–Washington University
Pediatric Cancer Genome Project

NEUROBLASTOMA, A TUMOR OF the sympathetic nervous system, is the most common extracranial solid tumor of childhood and accounts for 15% of all cancer-related deaths in children. Through the 1980s, deaths from neuroblastoma were usually an early event and less than 5% occurred beyond 3 years from diagnosis and less than 1% occurred

Context Neuroblastoma is diagnosed over a wide age range from birth through young adulthood, and older age at diagnosis is associated with a decline in survivability.

Objective To identify genetic mutations that are associated with age at diagnosis in patients with metastatic neuroblastoma.

Design, Setting, and Patients Whole genome sequencing was performed on DNA from diagnostic tumors and their matched germlines from 40 patients with metastatic neuroblastoma obtained between 1987 and 2009. Age groups at diagnosis included infants (0- <18 months), children (18 months- <12 years), and adolescents and young adults (≥12 years). To confirm the findings from this discovery cohort, validation testing using tumors from an additional 64 patients obtained between 1985 and 2009 also was performed. Formalin-fixed, paraffin-embedded tumor tissue was used for immunohistochemistry and fluorescence in situ hybridization. Telomere lengths were analyzed using whole genome sequencing data, quantitative polymerase chain reaction, and fluorescent in situ hybridization.

Main Outcome Measure Somatic recurrent mutations in tumors from patients with neuroblastoma correlated with the age at diagnosis and telomere length.

Results In the discovery cohort (n=40), mutations in the *ATRX* gene were identified in 100% (95% CI, 50%-100%) of tumors from patients in the adolescent and young adult group (5 of 5), in 17% (95% CI, 7%-36%) of tumors from children (5 of 29), and 0% (95% CI, 0%-40%) of tumors from infants (0 of 6). In the validation cohort (n=64), mutations in the *ATRX* gene were identified in 33% (95% CI, 17%-54%) of tumors from patients in the adolescent and young adult group (9 of 27), in 16% (95% CI, 6%-35%) of tumors from children (4 of 25), and in 0% (95% CI, 0%-24%) of tumors from infants (0 of 12). In both cohorts (N=104), mutations in the *ATRX* gene were identified in 44% (95% CI, 28%-62%) of tumors from patients in the adolescent and young adult group (14 of 32), in 17% (95% CI, 9%-29%) of tumors from children (9 of 54), and in 0% (95% CI, 0%-17%) of tumors from infants (0 of 18). *ATRX* mutations were associated with an absence of the *ATRX* protein in the nucleus and with long telomeres.

Conclusion *ATRX* mutations were associated with age at diagnosis in children and young adults with stage 4 neuroblastoma.

Trial Registration clinicaltrials.gov Identifier: NCT00588068

JAMA. 2012;307(10):1062-1071

www.jama.com

after 5 years.^{1,2} Survival for longer than 30 months after recurrence of stage 4 neuroblastoma was the exception, even with myeloablative retrieval therapy.³ During the 1990s, several studies began to describe late recurrences of neuroblastoma starting at 4 to 13 years from diagnosis, with some patients continuing to survive for

up to 19 years from diagnosis.⁴ Time to death after tumor recurrence among adolescents was significantly longer than

Author Affiliations are listed at the end of this article.
Corresponding Author: Michael A. Dyer, PhD, Department of Developmental Neurobiology, MS 323, St Jude Children's Research Hospital, 262 Danny Thomas Pl, Memphis, TN 38105 (michael.dyer@stjude.org).

among children. This difference was most evident for patients with advanced stage neuroblastoma.

Half of the patients (50%) with neuroblastoma present with metastatic disease; with current treatment approaches, the age at diagnosis has proven to be one of the most powerful predictors of outcome.⁵ The probability of overall survival is 88% in infants (age: <18 months at time of diagnosis), 49% in children (age: 18 months-<12 years), and only 10% in adolescents or young adults (age: ≥12 years).^{6,7} A majority of neuroblastoma occurring in adolescents and young adults as well as in some older children have a protracted course, with death occurring many years after diagnosis.^{8,9} This clinical subtype is now referred to as indolent or chronic neuroblastoma.⁴

Genetic mutations associated with neuroblastoma and its clinical course are not completely understood. To define the mutational landscape of metastatic neuroblastoma, the St Jude Children's Research Hospital–Washington University Pediatric Cancer Genome Project performed whole genome sequence analysis of DNA from tumors and matched germline samples from 40 pediatric patients with metastatic neuroblastoma diagnosed and/or treated at Memorial Sloan-Kettering Cancer Center (MSKCC). Tumors from patients diagnosed as infants, children, and adolescents and young adults were included.

METHODS

Patients and Tissues

The use of human tissues for our genetic studies was approved by the institutional review boards of MSKCC, St Jude Children's Research Hospital, and Washington University in St Louis. Written informed consent was obtained from patients or legal guardians at the time of the surgical resection or bone marrow procedure.

All patients diagnosed with metastatic neuroblastoma at MSKCC had tumor samples stored in the tumor inventory. From a pool of 158 available tumor samples diagnosed across all ages, tumor samples were selected at

random to represent each of the 3 patient diagnostic age groups for both a discovery cohort (n=40) and a validation cohort (n=64). The proportion of samples from each of the 3 age groups was not chosen to be representative of the relative frequency of metastatic neuroblastoma in those age groups, and no preference was given to sex, race/ethnicity, or clinical outcome. When the tumors passed pathology review for adequate tumor content (>50%) and adequate DNA quality, they were entered into the discovery cohort (n=40), and subsequently into the validation cohort (n=64). In addition, 1 patient from another institution had tissue submitted for evaluation in the validation cohort, which was approved for molecular studies under a waiver from that institution's institutional review board.

Patients were diagnosed between 1987 and 2009 for the discovery cohort and between 1985 and 2009 for the validation cohort. Information on age at diagnosis, sex, race/ethnicity, tumor stage, and survival were taken from the clinical database. Information on race/ethnicity was provided by the patient or parent and was included because some single nucleotide polymorphisms are differentially distributed across different populations.

Fresh tumor samples were cryopreserved at the time of surgery. Remission bone marrow or blood samples were cryopreserved to serve as a matched germline reference for each tumor. Formalin-fixed, paraffin-embedded tumor samples were used for immunohistochemistry and fluorescence in situ hybridization (FISH) studies. Whole genome sequencing (WGS) was performed on the discovery cohort to identify genetic lesions. Polymerase chain reaction (PCR) and Sanger sequencing were then performed on both the discovery and validation cohorts to validate somatic lesions. In addition, the association between age group and identified mutations was examined.

In addition, telomere analysis was performed in the discovery cohort because telomere length has been asso-

ciated with outcomes in patients with neuroblastoma. Mutations of *ATRX* were recently identified in pancreatic neuroendocrine tumors and were shown to be associated with lengthened telomeres generated by a mechanism known as alternative lengthening of telomeres (ALT).¹⁰ We also determined if neuroblastoma tumors with *ATRX* mutations had longer telomeres.

Whole Genome Sequencing

Using a paired-end sequencing approach, we sequenced DNA from the tumors and matching germline controls in the discovery cohort with an average of 35.1× haploid coverage per genome. Single nucleotide variations and insertions and deletions were identified as previously described.^{11,12} Structural variations were detected using the clipping reveals structure (CREST) algorithm.¹³ The WGS data are deposited at the European Bioinformatics Institute with accession number EGAS00001000213 (<https://www.ebi.ac.uk/ega/studies/EGAS00001000213>).

Sequence Validation

Polymerase chain reaction and Sanger sequencing were performed to validate somatic lesions in the discovery and validation cohorts. Polymerase chain reaction amplification was performed for 35 cycles using Advantage 2 polymerase (Clontech) with an annealing temperature of 68°C. A 5-μL sample of the resulting PCR product was purified using 2-μL ExoSAP-IT (Affymetrix) prior to Sanger sequencing. Polymerase chain reaction primer sequences are available upon request.

MYCN Copy Number Analysis

Amplification of *MYCN* was based on 3 independent methods: (1) review of the clinical database in which amplification was determined by Southern blotting or by FISH, (2) quantitative PCR using previously published methods,¹⁴ and (3) by WGS. All 3 methods gave identical results. For samples in which the *MYCN* copy number was greater than 10, the number of genes

in the amplicon was derived from WGS. For samples with 10 copies or fewer of *MYCN*, the size of the amplified region was determined as focal (≤ 5 genes), large segment (> 5 genes), or chromosomal (whole gain of chromosome 2).

Telomere Analysis

Telomeres were analyzed in the discovery cohort using 3 different methods. The WGS data were analyzed for telomere length for all tumors and germline DNA in the discovery cohort. Quantitative PCR was performed to validate the results from WGS analysis for all 10 tumors in the discovery cohort with *ATRX* mutations and an additional 4 samples with wild-type *ATRX* to serve as controls. Telomere FISH was performed on all tissue samples in the discovery cohort that had available formalin-fixed, paraffin-embedded samples. All of the samples that were analyzed by telomere FISH also were analyzed for *ATRX* protein expression by immunohistochemistry.

Telomere length was predicted in silico by counting the number of next-generation sequencing reads containing the telomeric repeat sequence TTAGGG.¹⁵ The resulting number of reads was normalized to the average genomic coverage, and the difference in diagnostic and germline telomeric sizes was calculated. Telomere length was validated in vitro in neuroblastomas expressing an *ATRX* aberration as described previously.^{16,17} Briefly, 15 to 20 ng of diagnostic and germline whole genome-amplified DNA was subject to quantitative PCR using 2 sets of primers in separate reactions—1 to amplify telomeric sequence and 1 to amplify the common gene *36B4* (*RPLP0*). The cycle threshold values obtained were compared with those of 2 standard curves—a telomeric standard curve performed on known quantities of a telomeric 84-mer oligonucleotide and 1 curve using an oligomer of *36B4* (*RPLP0*). All reactions were performed in triplicate with both tumor and germline DNA and both assays on the same plate.

All reactions were performed using Brilliant III Ultra-Fast SYBR Green master mix (Agilent) on a Stratagene Mx3000 thermal cycler with a melting temperature of 60°C. This allowed us to determine the telomere length in kb per diploid genome.

The forward primer for telomere analysis was

5'-CGGTTTGGTTGGGTTTGGGT
TTGGGTTTGGGTTTGGGTT-3'

The reverse primer for telomere analysis was

5'-GGCTTGCCTTACCCTTACCC
TTACCCTTACCCTTACCC-3'

The forward primer for the internal control *36B4* (*RPL0*) gene was

5'-CAGCAAGTGGGAAGGTGTA
TCC-3'

The reverse primer for the internal control *36B4* (*RPL0*) gene was

5'-CCCATTCTATCATCAACGGG
TACAA-3'

The standard used to generate the standard curve for telomeres was

5'-(TTAGGG)₁₄-3'

The standard used to generate the standard curve for the internal control *36B4* (*RPL0*) was

5'-CAGCAAGTGGGAAGGTG
TAATCCGTCTCCACAGACAAGG
CCAGGACTCGTTTGTACCCGT
TGATGATAGAATGGG-3'

ATRX Immunohistochemistry

Formalin-fixed, paraffin-embedded tissues were cut into 4- μ m-thick sections and immunostained with a polyclonal antibody against *ATRX* (1:600; Sigma-Aldrich) by using heat-induced epitope retrieval and the Leica Polymer Refine Detection Kit (Leica Microsystems) on a Leica Bond system after 15-minute antibody incubation.

Telomere FISH

Interphase FISH was performed on 4- μ m-thick formalin-fixed, paraffin-embedded tissue sections. The Cy3-labeled TelG probe (PNAbio) was co-denatured with the target cells on a hotplate at 90°C for 12 minutes. The slides were incubated for 48 hours at 37°C and then washed in 4 M urea/2 \times SSC at 45°C for 5 minutes. Nuclei were counterstained with 200 ng/mL

of 4',6-diamidino-2-phenylindole (Vector Laboratories).

Statistical Analysis

Cytel Studio StatXact 9 software (Cytel Inc) was used for the analyses. The exact χ^2 test was used to examine the association between age group and *ATRX* mutation. *P* values of less than .05 were considered statistically significant; all reported *P* values were 2-sided. Proportions are reported with 95% Blyth-Still-Casella confidence intervals. No sample size calculation was performed because this was a retrospective exploratory study.

RESULTS

Whole Genome Sequencing

We performed WGS on a discovery cohort of 40 diagnostic neuroblastoma samples from infants ($n=6$), children ($n=29$), and adolescents and young adults ($n=5$) with stage 4 disease. Patient characteristics are presented in TABLE 1 and eTable 1 and eTable 2 at <http://www.jama.com>. Somatic mutations in *ATRX*, including sequence mutations and structural variations, were found in 25% (95% CI, 13%-41%) of the tumors (10 of 40). Three of the mutations were missense mutations (*L407F*, *A1690D*, and *R2188Q*), 1 of the mutations was a nonsense mutation (*E555**), 1 was a frameshift mutation (*K425-fs*), and the remaining 5 mutations were structural variations resulting in an in-frame deletion in *ATRX* protein (FIGURE 1). The minimum overlapping region of the deletion involved exon 5 to exon 10, which encodes a predicted nuclear localization signal (Figure 1). All 10 somatic mutations were validated by PCR and Sanger sequencing. *ATRX* mutations were mutually exclusive of *MYCN* amplification in the discovery cohort (eTable 2).

ATRX is on the X chromosome and 7 of the 10 patients with *ATRX* mutations were males and would thus only have a mutant allele (eTable 1). One of the females with an *ATRX* mutation also sustained a loss of 1 copy of the X chromosome in the tumor, thereby eliminating the wild-type allele of *ATRX* (eTable 1).

The remaining 2 females with *ATRX* mutations were diagnosed as children (at 2.3 and 4.1 years of age) and had heterozygous in-frame deletions (Table 1 and eTable 1).

Telomere Analysis

Among the 10 patients whose tumors had *ATRX* mutations, 8 had evidence of longer telomeres (80%; 95% CI, 44%-96%) based on WGS data (TABLE 2 and FIGURE 2A). In contrast, only 40% (95% CI, 24%-59%) of the tumors with wild-type *ATRX* had long telomeres (12 of 30; Table 1 and Table 2), although the difference was not statistically significant ($P=.07$). Each of the 8 tumors that showed evidence of longer telomeres by WGS analysis was validated using the quantitative PCR method; 1 of 2 samples with short telomeres by WGS had longer telomeres by the quantitative PCR method (Figure 2C and eTable 2). As expected, the 4 samples with wild-type *ATRX* showed consistent results between the WGS and quantitative PCR analysis (eTable 2).

Telomere FISH analysis was performed on 28 patients in the discovery cohort that had available formalin-fixed, paraffin-embedded tumor specimens (eTable 2). All 8 of the *ATRX* mutant tumors that had long telomeres from WGS and quantitative PCR contained a large ultrabright telomere FISH signal that is a hallmark of ALT^{18,19} (FIGURE 3 and eTable 2). Only 1 of the 20 tumors with wild-type *ATRX* had evidence of ALT (eTable 2).

ATRX Protein Localization

All 8 of the samples with *ATRX* mutations among the 28 with available tissue blocks had complete or mosaic loss of the nuclear *ATRX* protein (eTable 1 at <http://www.jama.com> and FIGURE 4). Only 1 of the 20 tumor samples with wild-type *ATRX* had mosaic loss of the *ATRX* protein in the nucleus (eTable 1). This sample did not have any evidence of ALT (eTable 1).

Age Association

All 5 samples from adolescents and young adult patients in the discovery

Table 1. Patient Characteristics

	No. (%) of Patients ^a		
	All Patients (N = 104)	Discovery Cohort (n = 40)	Validation Cohort (n = 64)
Sex			
Male	57 (55)	26 (65)	31 (48)
Female	47 (45)	14 (35)	33 (52)
Race/ethnicity			
White, non-Hispanic	72 (69)	30 (75)	42 (66)
White, Hispanic	2 (2)	1 (3)	1 (2)
Black, non-Hispanic	15 (14)	6 (15)	9 (14)
Black, Hispanic	1 (1)	1 (3)	0
Asian, Far East, or Indian subcontinent	3 (3)	1 (3)	2 (3)
Unknown	10 (10)	1 (3)	9 (14)
Other ^b	1 (1)	0	1 (2)
Stage			
2B, then 4	1 (1)	1 (3)	0
3, then 4	1 (1)	0	1 (2)
4s, then 4	1 (1)	1 (3)	0
3	1 (1)	0	1 (2)
4	100 (96)	38 (95)	62 (97)
Age at diagnosis			
<18 mo	18 (17)	6 (15)	12 (19)
≥18 mo-<12 y	54 (52)	29 (73)	25 (39)
≥12 y	32 (31)	5 (13)	27 (42)
<i>MYCN</i> amplification			
Amplified	24 (23)	11 (28)	13 (20)
Not amplified	80 (77)	29 (73)	51 (80)
<i>ATRX</i> mutation or deletion			
Yes	23 (22)	10 (25)	13 (20)
No	81 (78)	30 (75)	51 (80)
<i>ALK</i> mutation			
Yes	15 (14)	6 (15)	9 (14)
No	89 (86)	34 (85)	55 (86)
Telomere length ^c			
Long	NA	20 (50)	NA
Short	NA	20 (50)	NA
11q			
Loss	NA	18 (45)	NA
Gain	NA	3 (8)	NA
No change	NA	19 (48)	NA
1p			
Loss	NA	17 (43)	NA
Gain	NA	4 (10)	NA
No change	NA	17 (43)	NA
Weak loss ^d	NA	1 (3)	NA
Weak gain ^d	NA	1 (3)	NA
17q			
Gain	NA	36 (90)	NA
No change	NA	4 (10)	NA
Relapse or progression			
Yes	78 (75)	28 (70)	50 (78)
No	26 (25)	12 (30)	14 (22)
Survival status			
Dead	58 (56)	21 (53)	37 (58)
Alive	46 (44)	19 (48)	27 (42)

Abbreviation: NA, not applicable.

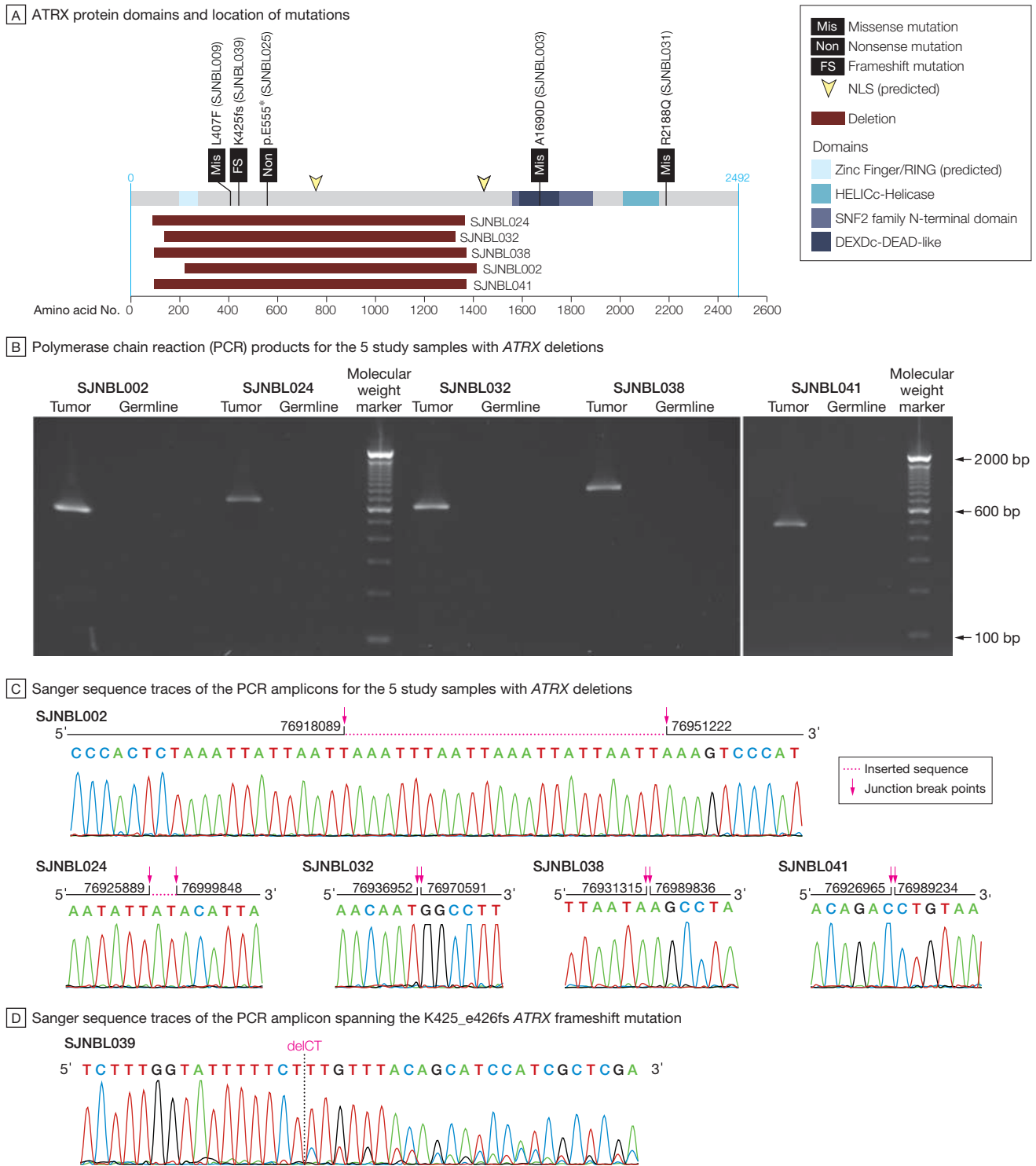
^aPercentages may not sum to 100% due to rounding.

^bIncludes patients whose race/ethnicity did not fit into 1 of the categories listed.

^cCalculated from the genomic reads that correspond to the telomere sequence from the tumor and the matched germline as follows: (No. of telomere reads in tumor - No. of telomere reads in the germline sample)/No. of telomere reads in the germline sample. To be classified as long, this value must be greater than 0.05; short, less than -0.05.

^dWeak loss: 0.25 to 0.75 copies; weak gain: 0.25 to 0.75 copies.

Figure 1. ATRX Mutations in Neuroblastoma



A, Diagram of the ATRX protein and changes that result from the 5 single nucleotide variations and 5 in-frame deletions found in the ATRX gene. B, Ethidium bromide-stained agarose gel with the PCR products for each of the 5 deletions shown in panel A. C, Sanger sequence traces of the PCR amplicons from panel B with junction break points (arrows). D, Sanger sequence traces of the PCR amplicon spanning the frameshift mutation K425_E426fs. NLS indicates nuclear localization signal.

cohort had *ATRX* mutations (100%; 95% CI, 50%-100%), whereas no *ATRX* mutations were detected in 6 samples obtained from infants (0%; 95% CI, 0%-40%) (TABLE 3). Among the 29 children aged 18 months to 12 years, *ATRX* mutations were identified in 5 (17%; 95% CI, 7%-36%), with 4 of 5 patients living at least twice as long as their time to first relapse, similar to most indolent neuroblastoma seen in the adolescent and young adult group (eTable 1). A significant association ($P < .001$) was observed for the discovery cohort between *ATRX* mutation and age group.

Validation Cohort

We analyzed the *ATRX* gene in tumors from an additional 64 patients with neuroblastoma (12 from infants, 25 from children, and 27 from adolescents and young adults; Table 3 and eTable 3). We identified 13 additional *ATRX* mutations in children ($n=4$) and adolescents and young adults ($n=9$) (eTable 3). No *ATRX* mutations were identified in infants from the validation cohort. The children with *ATRX* mutations were all older than 5 years at the time of diagnosis and 1 of the 3 who died had a protracted disease course (eTable 3). A significant association ($P = .048$) was observed between *ATRX* mutation and age of disease diagnosis (Table 3). When the discovery cohort and validation cohort were combined, this age association was also significant ($P < .001$).

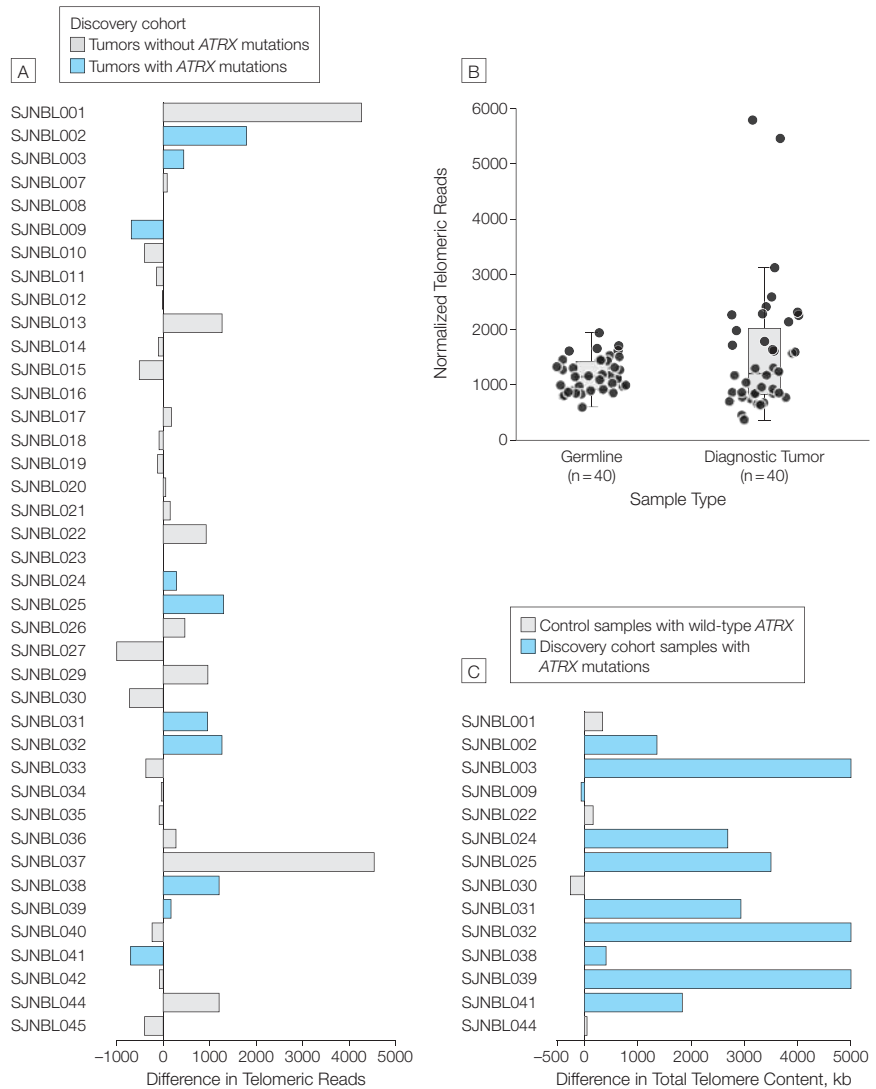
COMMENT

In this study, *ATRX* mutations were found in 44% (95% CI, 28%-62%) of tumors from adolescent and young adult patients with metastatic neuroblastoma and none of the tumors (0%; 95% CI, 0%-17%) from infants with metastatic neuroblastoma. The children whose tumors had *ATRX* mutations were typically older than 5 years or had a chronic or indolent course of disease. The *ATRX* mutations were characterized as missense, nonsense, frameshift, or in-frame deletion and they were mutually exclusive of *MYCN* amplification. *ATRX* mutations were as-

Table 2. *ATRX* and Telomere Results for the Discovery Cohort ($n = 40$)

	<i>ATRX</i> Mutation		<i>P</i> Value
	Yes ($n = 10$)	No ($n = 30$)	
Telomere length, No. (%) [95% CI]			
Long	8 (80) [44-96]	12 (40) [24-59]	.07
Short	2 (20) [4-56]	18 (60) [41-76]	

Figure 2. Telomere Analysis in Neuroblastoma



A, Difference in telomeric reads for each of the 40 tumors in the discovery cohort based on the whole genome sequencing data. The reference value for each tumor was the telomere length from matched normal DNA from the same patient. The actual value for SJNBL008 was -57 ; SJNBL016, -39 ; and SJNBL023, 27 . B, Box plot of normalized telomeric reads for the germline DNA and the diagnostic tumor from whole genome sequencing data for the 40 tumors and matched germline samples in the discovery cohort. The number of telomeric reads was normalized to the average genomic coverage for that particular sample. The upper and lower edges of the box represent the 75th and 25th percentile, respectively. The median is indicated as a horizontal line within the box and the error bars represent the lowest and highest values still within 1.5 of the interquartile range. C, Quantitative polymerase chain reaction for telomeres in the 10 samples in the discovery cohort with *ATRX* mutations as well as 4 controls with wild-type *ATRX*. Data are plotted as difference between tumor and germline for each patient. The actual value for SJNBL003 was 10939; SJNBL032, 8171; and SJNBL039, 10612.

sociated with loss of the nuclear ATRX protein, longer telomeres, and ALT. Unlike pancreatic neuroendocrine tumors, which are associated with a high frequency of *ATRX* and *DAXX* mutations, we did not detect any *DAXX* mutations in neuroblastomas.

These results suggest that inactivation of the *ATRX* pathway correlates with older age at diagnosis and may provide a molecular marker and potential therapeutic target for neuroblastoma among adolescents and young adults. It may also delineate the subset of children with neu-

roblastoma who have a chronic but progressive clinical course. Specifically, patients with *ATRX* mutations, ultrabright telomere FISH signals characteristic of ALT, loss of nuclear ATRX proteins, and absence of *MYCN* gains may be more likely to have a chronic but progressive clinical course when receiving standard therapeutic approaches and may require a different treatment strategy.

ATRX Function

ATRX is part of a multiprotein complex that includes *DAXX* and plays a role in

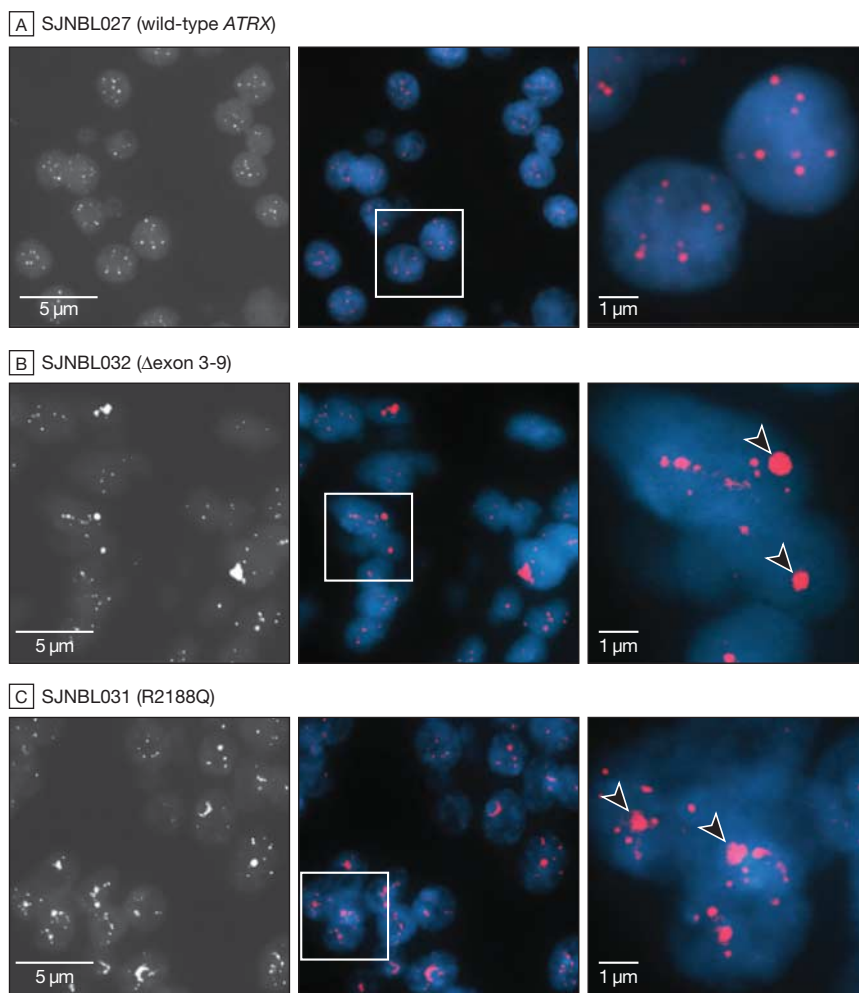
regulating adenosine triphosphate-dependent chromatin remodeling, nucleosome assembly, and telomere maintenance. ATRX has been extensively studied in the α -thalassemia/mental retardation X-linked syndrome.²⁰ It is thought that mutations in patients with this syndrome retain partial activity of ATRX. In contrast, the identified *ATRX* mutations in pancreatic neuroendocrine tumors and neuroblastomas, as well as the *DAXX* mutations seen in pancreatic neuroendocrine tumors, appear to be loss-of-function mutations. How these alterations lead to lengthened telomeres remains to be determined.

Beyond the proposed role in telomere maintenance, ATRX is also believed to play a role in epigenetic regulation of gene expression by controlling the deposition of histone H3.3 at transcriptionally silent regions of the genome.²¹⁻²⁴ This may lead to increased expression of oncogenes in tumors with *ATRX* mutations through epigenetic mechanisms.

Long-term Survival, ATRX, and ALT

In patients with neuroblastoma, the short-term survival for the adolescent and young adult group of patients is better than among children, but the overall survival is worse. This reflects the chronic or indolent disease progression in this older age group. Among 68 patients with pancreatic neuroendocrine tumors, 29 had mutations (42.6%) in *ATRX* or *DAXX* and those mutations were associated with prolonged survival at 5 years after diagnosis.²⁵ However, all of the patients with *ATRX* and *DAXX* mutations died by 15 years postdiagnosis, which is similar to the poor long-term outcome for adolescents and young adults with neuroblastoma. Although it is not yet known if the overall survival for patients with pancreatic neuroendocrine tumors carrying the wild-type *ATRX*/*DAXX* is better than those with *ATRX*/*DAXX* mutations by 15 years postdiagnosis, it is a testable hypothesis that mutations in the *ATRX*/*DAXX* pathway may dictate a slower-growth tumor in the short-term, but in time they ultimately contribute to death.

Figure 3. Telomere Analysis in 3 Representative Neuroblastoma Samples



Images of cells with wild-type *ATRX* (A) and 2 samples with mutant *ATRX* (B and C) hybridized with the telomere fluorescent in situ hybridization probe (red) and stained with 4',6-diamidino-2-phenylindole (blue) to visualize the nuclei. Left panels, grayscale images of the telomere fluorescence in situ hybridization signal; middle panels, low-power overlay images; right panels, high-magnification views highlighting the large ultrabright signals (arrowheads) in the *ATRX* mutant neuroblastoma cells.

ATRX and Neuroblastoma

Despite detailed clinical descriptions,^{26,27} the definition of chronic or indolent neuroblastoma has been imprecise and sometimes inconsistent for optimal patient care. Because these tumors can respond differently to induction chemotherapy, stem cell transplant, and antibody therapy, their inclusion in small pilot studies may be misleading, especially when stable disease is used as the treatment end point. While the age of 12 years at diagnosis is a convenient cutoff, it is now recognized that patients in the younger age group also may have a chronic or indolent clinical course. Unfortunately, their distinction from the rest of children with neuroblastoma is nearly always in retrospect. The absence of a thorough understanding of the molecular or genetic biology of this subset makes it difficult to identify and optimally treat these patients.

MYCN amplification and *ALK* mutations are among the most prevalent and biologically important genetic aberrations in neuroblastoma.^{28,29} The oncogenic potential of *MYCN* is well-known.³⁰ While *MYCN* amplification is generally found in high-risk tumors, *ALK* mutation is equally represented among patients with low-stage or advanced-stage disease. In fact, germline *ALK* mutations are responsible for a subset of patients with hereditary neuroblastoma.²⁹ The identification of *ATRX* mutations now provides a new biomarker that may assist in identifying patients who develop a chronic but progressive clinical course, and thus may be candidates for altered risk-based therapies.^{6,31}

Strengths and Limitations

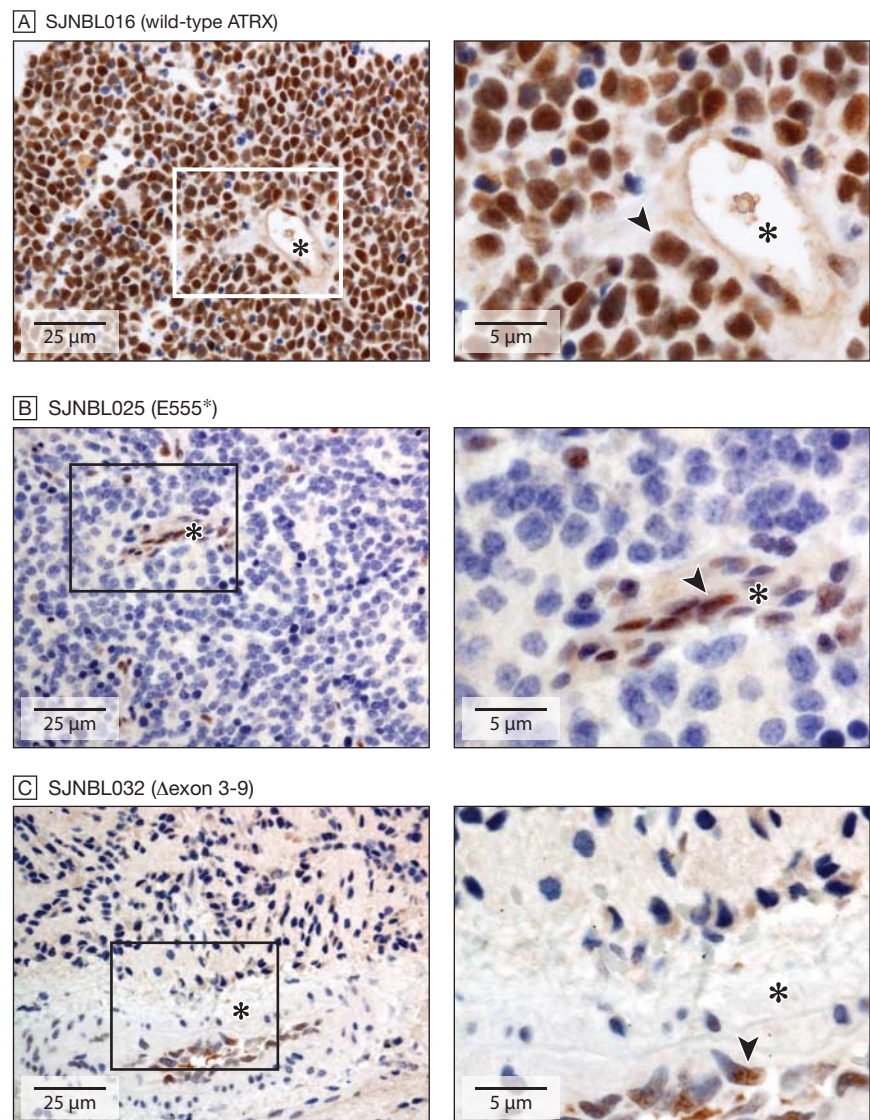
The major strength of our study is the relatively large sample size of patients with stage 4 neuroblastoma representing the 3 major age groups of this disease. Most of the other genetic or genomic studies on neuroblastoma have focused on younger patients. Our analysis of infants, children, adolescents, and young adults from the same institution diagnosed during the same pe-

riod provided us with the unique opportunity to identify genetic lesions associated with age at diagnosis for neuroblastoma. The other strength of our study is the use of WGS in the discovery cohort. This provided an opportunity to identify both structural variations and sequence mutations in *ATRX*. These variations, which result in focal

deletions, may be difficult to identify by single nucleotide polymorphism array analysis or exome capture approaches.

In this study, we used the Illumina paired-end sequencing technology to generate sequencing reads from short DNA fragments of the tumor and matched normal cells. This massively

Figure 4. Immunohistochemistry for ATRX Protein Expression in 3 Representative Neuroblastoma Samples



A, Immunohistochemistry for ATRX protein (brown) in a neuroblastoma tumor with wild-type *ATRX*. Hematoxylin counterstain stains the unlabeled (*ATRX* negative) nuclei blue. Blood vessels are clearly visible (*). The arrowhead indicates nuclear staining of ATRX. B and C, Immunohistochemistry for ATRX protein on 2 neuroblastoma samples with *ATRX* mutations. The vascular endothelial cells lining the blood vessel (*) are immunopositive for ATRX (arrowheads) but the tumor cells are negative.

Table 3. Genetic and Telomere Results by Age Group

	No. (%) [95% CI]			P Value
	Infants (Age: <18 mo) (n = 18)	Children (Age: 18 mo-<12 y) All Patients (N = 104) (n = 54)	Adolescents and Young Adults (Age: ≥12 y) (n = 32)	
<i>ATRX</i> mutation				
Yes	0 (0) [0-17]	9 (17) [9-29]	14 (44) [28-62]	<.001
No	18 (100) [83-100]	45 (83) [71-91]	18 (56) [38-72]	
	(n = 6)	Discovery Cohort (n = 40) (n = 29)	(n = 5)	
<i>ATRX</i> mutation				
Yes	0 (0) [0-40]	5 (17) [7-36]	5 (100) [50-100]	<.001
No	6 (100) [60-100]	24 (83) [64-93]	0 (0) [0-50]	
Telomere length ^a				
Long	5 (83) [40-99]	11 (38) [21-58]	4 (80) [34-99]	.05
Short	1 (17) [1-60]	18 (62) [42-79]	1 (20) [1-66]	
	(n = 12)	Validation Cohort (n = 64) (n = 25)	(n = 27)	
<i>ATRX</i> mutation				
Yes	0 (0) [0-24]	4 (16) [6-35]	9 (33) [17-54]	.048
No	12 (100) [76-100]	21 (84) [65-94]	18 (67) [46-83]	

^aData were available only for this cohort.

parallel sequencing technology provides multiple DNA sequencing reads across individual nucleotides in the genome. The average number of sequencing reads for each nucleotide (coverage) for the 40 tumors and 40 matched germline samples was $35.1 \times$ (range, $26.7 \times$ to $46.5 \times$). This coverage ensures that an average of 98.5% (96.1%-99.6%) of genomic regions and 93.3% (85.0%-98.8%) of exonic regions were covered by at least 10 high-quality sequence reads, which is sufficient to identify somatic mutations. However, one of the limitations of the current study is the possibility that a small proportion of somatic mutations were missed due to insufficient coverage.

Another limitation of our study is the different methods used to analyze *ATRX* mutations in the discovery and validation cohorts. Our data on the discovery cohort are far more comprehensive than on the validation cohort because WGS was used for the discovery cohort whereas PCR and Sanger sequencing were used for the validation cohort. This may account for the lower rate of *ATRX* lesions in the validation cohort because the method used was not as sensitive in detecting deletions or low-

frequency single nucleotide variations. Also, we did not analyze the X-chromosome copy number in our validation cohort to determine if any of the females with *ATRX* mutations had lost all or part of the X chromosome. Similarly, we did not perform transcriptome sequencing for any of the samples in this study to determine if X inactivation contributes to inactivation of the wild-type allele of *ATRX* in female patients.

Future studies should focus on assembling larger international cohorts of patients to study the short-term and long-term outcomes for patients with neuroblastoma across all age groups with *ATRX* mutations compared with those without *ATRX* mutations. These data may be useful in defining a more relevant age cutoff for the adolescent and young adult group and help to identify more effectively those patients who will have an increased risk of developing chronic or indolent neuroblastoma. Moreover, future studies should focus on exploring novel therapeutics for treating patients with *ATRX* mutations and the mechanistic connection between perturbations in this pathway, ALT, changes in gene expression that result from defects in histone H3.3 deposi-

tion, and the unique form of disease found in these patients.

CONCLUSIONS

This analysis of the *ATRX* gene in 104 patients with advanced-stage neuroblastoma provides age-group-specific data on the frequency of *ATRX* pathway disruption and ALT. Additional studies with larger cohorts of patients will be required to determine if genetic analysis of *ATRX* mutation status in children will be useful to prospectively identify children likely to develop chronic or indolent neuroblastoma.

Author Affiliations: Departments of Pediatrics (Drs N-K. Cheung and I. Cheung), Pathology (Dr Tickoo), and Human Oncology and Pathogenesis (Dr Heguy), Memorial Sloan-Kettering Cancer Center, New York, New York; Departments of Computational Biology (Drs Zhang, Parker, and Chen), Pathology (Drs Bahrami, Ellison, and Downing and Mr Dalton), Oncology (Drs Pappo and Federico), Biostatistics (Dr Wu and Ms Bil-lups), Developmental Neurobiology (Dr Dyer), and the Hartwell Center for Bioinformatics and Biotechnology (Dr Wang and Mr Becksfors), St Jude Children's Research Hospital, Memphis, Tennessee; The Genome Institute (Drs Lu, Ding, and Mardis and Mr Fulton); Department of Genetics (Dr Mardis) and Siteman Cancer Center (Drs Mardis and Wilson), Washington University School of Medicine, St Louis, Missouri; Department of Ophthalmology, University of Tennessee Health Science Center, Memphis (Dr Dyer); and Howard Hughes Medical Institute, Chevy Chase, Maryland (Dr Dyer).

Author Contributions: Dr Dyer had full access to all of the data in the study and takes responsibility for

the integrity of the data and the accuracy of the data analysis. Drs N-K. Cheung, Zhang, and Lu contributed equally to the work.

Study concept and design: N-K. Cheung, Zhang, Tickoo, Pappo, Mardis, Wilson, Downing, Dyer.

Acquisition of data: N-K. Cheung, Zhang, Parker, Bahrami, Tickoo, Heguy, Federico, I. Cheung, Ding, Fulton, Ellison, Wilson.

Analysis and interpretation of data: N-K. Cheung, Zhang, Lu, Parker, Bahrami, Heguy, Pappo, Federico, Dalton, Ding, Wang, Chen, Becksfort, Wu, Billups, Ellison, Mardis, Wilson, Downing, Dyer.

Drafting of the manuscript: N-K. Cheung, Zhang, Parker, Bahrami, Heguy, Pappo, Federico, Dalton, Wu, Billups, Ellison, Downing, Dyer.

Critical revision of the manuscript for important intellectual content: N-K. Cheung, Zhang, Lu, Tickoo, Pappo, Federico, I. Cheung, Ding, Fulton, Wang, Chen, Becksfort, Mardis, Wilson, Downing, Dyer.

Statistical analysis: Zhang, Lu, Parker, Chen, Becksfort, Wu, Billups.

Obtained funding: N-K. Cheung, Wilson, Downing.

Administrative, technical, or material support:

N-K. Cheung, Heguy, Federico, Dalton, I. Cheung, Fulton, Chen, Becksfort, Ellison, Mardis, Wilson, Downing, Dyer.

Study supervision: N-K. Cheung, Zhang, Pappo, Ding, Mardis, Wilson, Downing, Dyer.

Conflict of Interest Disclosures: The authors have completed and submitted the ICMJE Form for Disclosure of Potential Conflicts of Interest. Dr N-K. Cheung reported holding patents for monoclonal antibodies, beta-glucan, GD2 peptide mimetics, and methods for detecting residual disease and receiving royalties from United Therapeutics and Biotech Pharmacion. Dr Pappo reported serving as a consultant to Ziopharm. No other author reported disclosures.

Funding/Support: The whole genome sequencing was supported as part of the St Jude Children's Research Hospital-Washington University Pediatric Cancer Genome Project. This work was supported in part by Cancer Center Support grant CA21765 from the National Cancer Institute; grants EY014867 and EY018599 from the National Institutes of Health (awarded to Dr Dyer); and the American Lebanese Syrian Associated Charities of

St Jude Children's Research Hospital. Dr Dyer is a Howard Hughes Medical Institute Early Career Scientist. This work also was supported by the Catie Hoch Foundation and the Robert Steel Foundation.

Role of the Sponsors: None of the funding sources played any role in the design and conduct of the study; collection, management, analysis, and interpretation of the data; and preparation, review, or approval of the manuscript.

Online-Only Material: eTables 1 through 3 are available at <http://www.jama.com>.

Additional Contributions: Michael Rusch, BS (St Jude Children's Research Hospital) provided annotation of the focal deletions identified in *ATRX*. Robert Huether, PhD (St Jude Children's Research Hospital) provided interpretation of the functional impact of the *ATRX* mutations based on protein structure modeling. Clayton Naeve, PhD (St Jude Children's Research Hospital) provided computational infrastructure for data analysis. Elizabeth Chamberlain, BA (Memorial Sloan-Kettering Cancer Center) provided assistance with clinical data management. No compensation was provided to the individuals listed in this section.

REFERENCES

- Bowman LC, Hancock ML, Santana VM, et al. Impact of intensified therapy on clinical outcome in infants and children with neuroblastoma: the St Jude Children's Research Hospital experience, 1962 to 1988. *J Clin Oncol*. 1991;9(9):1599-1608.
- Cotterill SJ, Pearson AD, Pritchard J, et al. Clinical prognostic factors in 1277 patients with neuroblastoma: results of the European Neuroblastoma Study Group "Survey" 1982-1992. *Eur J Cancer*. 2000;36(7):901-908.
- Ladenstein R, Lasset C, Hartmann O, et al. Impact of megatherapy on survival after relapse from stage 4 neuroblastoma in patients over 1 year of age at diagnosis: a report from the European Group for Bone Marrow Transplantation. *J Clin Oncol*. 1993;11(12):2330-2341.
- Kushner BH, Kramer K, Cheung NK. Chronic neuroblastoma. *Cancer*. 2002;95(6):1366-1375.
- Moroz V, Machin D, Faldum A, et al. Changes over three decades in outcome and the prognostic influence of age-at-diagnosis in young patients with neuroblastoma: a report from the International Neuroblastoma Risk Group Project. *Eur J Cancer*. 2011;47(4):561-571.
- Cohn SL, Pearson AD, London WB, et al; INRG Task Force. The International Neuroblastoma Risk Group (INRG) classification system: an INRG Task Force report. *J Clin Oncol*. 2009;27(2):289-297.
- Franks LM, Bollen A, Seeger RC, Stram DO, Matthay KK. Neuroblastoma in adults and adolescents: an indolent course with poor survival. *Cancer*. 1997;79(10):2028-2035.
- Kushner BH, Kramer K, LaQuaglia MP, Modak S, Cheung NK. Neuroblastoma in adolescents and adults: the Memorial Sloan-Kettering experience. *Med Pediatr Oncol*. 2003;41(6):508-515.
- Conte M, Parodi S, De Bernardi B, et al. Neuroblastoma in adolescents: the Italian experience. *Cancer*. 2006;106(6):1409-1417.
- Heaphy CM, de Wilde RF, Jiao Y, et al. Altered telomeres in tumors with *ATRX* and *DAXX* mutations. *Science*. 2011;333(6041):425.
- Zhang J, Benavente CA, McEvoy J, et al. A novel retinoblastoma therapy from genomic and epigenetic analyses. *Nature*. 2012;481(7381):329-334.
- Zhang J, Ding L, Holmfeldt L, et al. The genetic basis of early T-cell precursor acute lymphoblastic leukaemia. *Nature*. 2012;481(7380):157-163.
- Wang J, Mullighan CG, Easton J, et al. CREST maps somatic structural variation in cancer genomes with base-pair resolution. *Nat Methods*. 2011;8(8):652-654.
- Anderson J, Gibson S, Williamson D, et al. Rapid and accurate determination of *MYCN* copy number and 1p deletion in neuroblastoma by quantitative PCR. *Pediatr Blood Cancer*. 2006;46(7):820-824.
- Castle JC, Biery M, Bouzek H, et al. DNA copy number, including telomeres and mitochondria, assayed using next-generation sequencing. *BMC Genomics*. 2010;11:244.
- Cawthon RM. Telomere measurement by quantitative PCR. *Nucleic Acids Res*. 2002;30(10):e47.
- O'Callaghan N, Dhillon V, Thomas P, Fenech M. A quantitative real-time PCR method for absolute telomere length. *Biotechniques*. 2008;44(6):807-809.
- Hampton T. Studies probe role of telomere length in predicting, modulating cancer risk. *JAMA*. 2011;305(22):2278-2279.
- Pickett H, Reddel R. Alternative lengthening of telomeres in human cancer. In: Hiyama K, ed. *Telomeres and Telomerase in Cancer*. New York, NY: Humana; 2009.
- Gibbons R. Alpha thalassaemia-mental retardation, X linked. *Orphanet J Rare Dis*. 2006;1:15.
- Drané P, Ouararhni K, Depaux A, Shuaib M, Hamiche A. The death-associated protein *DAXX* is a novel histone chaperone involved in the replication-independent deposition of H3.3. *Genes Dev*. 2010;24(12):1253-1265.
- Goldberg AD, Banaszynski LA, Noh KM, et al. Distinct factors control histone variant H3.3 localization at specific genomic regions. *Cell*. 2010;140(5):678-691.
- Law MJ, Lower KM, Voon HP, et al. *ATR-X* syndrome protein targets tandem repeats and influences allele-specific expression in a size-dependent manner. *Cell*. 2010;143(3):367-378.
- Lewis PW, Elsaesser SJ, Noh KM, Stadler SC, Allis CD. *Daxx* is an H3.3-specific histone chaperone and cooperates with *ATRX* in replication-independent chromatin assembly at telomeres. *Proc Natl Acad Sci U S A*. 2010;107(32):14075-14080.
- Jiao Y, Shi C, Edil BH, et al. *DAXX/ATRX*, *MEN1*, and *mTOR* pathway genes are frequently altered in pancreatic neuroendocrine tumors. *Science*. 2011;331(6021):1199-1203.
- Pollock BH, Krischer JP, Vietti TJ. Interval between symptom onset and diagnosis of pediatric solid tumors. *J Pediatr*. 1991;119(5):725-732.
- Garaventa A, Parodi S, De Bernardi B, et al. Outcome of children with neuroblastoma after progression or relapse: a retrospective study of the Italian neuroblastoma registry. *Eur J Cancer*. 2009;45(16):2835-2842.
- Seeger RC, Brodeur GM, Sather H, et al. Association of multiple copies of the *N-myc* oncogene with rapid progression of neuroblastomas. *N Engl J Med*. 1985;313(18):1111-1116.
- Deyell RJ, Attiyeh EF. Advances in the understanding of constitutional and somatic genomic alterations in neuroblastoma. *Cancer Genet*. 2011;204(3):113-121.
- Weiss WA, Aldape K, Mohapatra G, Feuerstein BG, Bishop JM. Targeted expression of *MYCN* causes neuroblastoma in transgenic mice. *EMBO J*. 1997;16(11):2985-2995.
- London WB, Castel V, Monclair T, et al. Clinical and biologic features predictive of survival after relapse of neuroblastoma: a report from the International Neuroblastoma Risk Group project. *J Clin Oncol*. 2011;29(24):3286-3292.